DEVELOPMENT OF THE DEMOUNTABLE DAMPED CAVITY

T. Konomi[#], The Graduate University for Advanced Studies
F.Yasuda, The Graduate School of University of Tokyo
F. Furuta, Cornell University
K.Saito, KEK, High Energy Accelerator Research Organization Accelerator Laboratory

Abstract

We have designed a new HOM free cavity named Demountable Damped Cavity (DDC) as an ILC R&D. DDC has two design concepts. The first one is an axial symmetry to eliminate kick off effect by HOM coupler itself. DDC is applied coaxial structure along the beam axis to make strong coupling with HOMs. HOMs are damped in RF absorber at the end of coaxial waveguide and the accelerating mode is reflected by the choke filter mounted nearby the end cell. The second concept is demountable structure which can make cleaning the end group easy in order to suppress the Q-slope problem at high field. In this paper, we will report about a RF absorber shape, thermal structure, 9 Cell cavity shape and preliminary vertical test result on the single cell DDC structure.

INTRODUCTION

We are developing the Demountable Damped Cavity (DDC) as R&D of ILC main linac (Fig. 1). There are two features in DDC. One is the axial symmetry structure, which will eliminate the beam kick effect in the TESLA type HOM coupler [1]. The second feature is the demountable structure. It makes cleaning the end group easy in order to suppress the high field Q slope [2].We finished designing the choke cavity structure. We have designed the absorber shape.

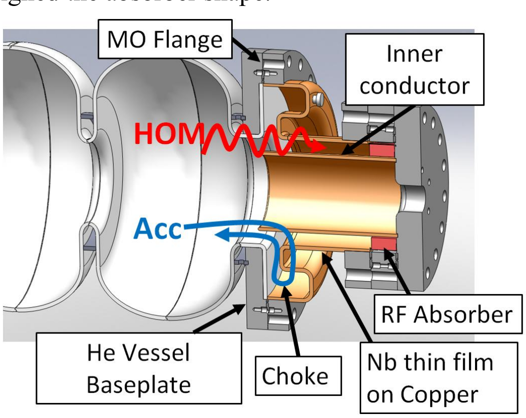

Fig. 1: The design of the DDC.

RF ABSORBER STRUCTURE

In the ILC main linac, the heat flux to 2K liquid helium has to be suppressed strictly. The RF absorber, which is mounted at the end of coaxial waveguide, is kept at 80K in our design. Data of absorber material parameter measured at 80K is very limited. We measured the Ni-Zn ferrite absorber (CMD10; Ceramic Magnetic Inc. [3]) at 80K. In the ILC 1.3GHz cavity, harmful HOMs are excited around 2~3 GHz. We designed DDC HOM damper shape mainly for those HOMs to be damped based on the measured data.

[#] konomi@post.kek.jp

Absorber Measurement System

We measured the complex permeability $\mu = \mu' + i\mu''$ and the complex permittivity $\varepsilon = \varepsilon' + i\varepsilon''$ of the ferrite at same time by the Nicolson-Ross-Weir method [4]. This is an easy method because reflection Γ and attenuation P can be measured by just inserting the sample in a transmission line.

$$\Gamma = \frac{\sqrt{\mu/\varepsilon} - 1}{\sqrt{\mu/\varepsilon} + 1} \tag{1}$$

$$P = \exp\left(-\frac{j\omega d}{c}\sqrt{\mu\varepsilon}\right) \tag{2}$$

, where ω is the angular frequency, d is the sample length, c is the speed of light.

We made a 50Ω coaxial waveguide sample holder (Fig. 2). It can keep the sample under vacuum to measure the RF property without any gas environment. The sample length is fixed 20mm, because the ferrite characteristic parameters dominate around 1MHz~1GHz. The measurement system was calibrated by measuring a copper sample with the same ferrite's shape and measuring empty sample holder. We confirmed our measurement system by measuring polyethylene's RF characteristics well known. Our result with polyethylene permittivity is ε=2.2±0.1, which is the same value with one reported already [5].

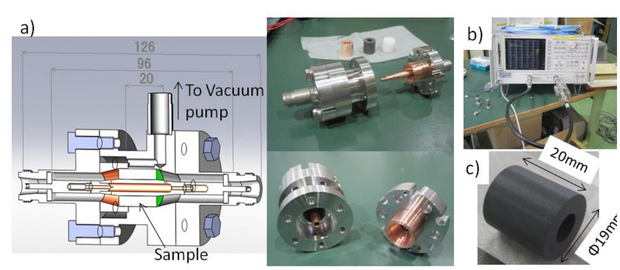

Fig. 2: Permeability and permittivity measurement system a) 50Ω coaxial sample holder b) Measurement view with Network Analyzer c) Ferrite sample.

Ni-Zn Ferrite (CMD10)

The permeability of ferrite consists of spin and domain wall [6]. The contributions from the spin and the domain wall are written as follows,

$$\mu = 1 + \frac{\mu_{s0}\omega_{s0}(\omega_{s0} + i\omega\alpha)}{(\omega_s + i\omega\alpha)^2 - \omega^2} + \frac{\mu_{d0}\omega_{d0}^2}{\omega_{d0}^2 + \omega + i\omega\beta}$$
$$\approx 1 + \frac{\mu_{s0}}{1 + i\omega/\omega_s} + \frac{\mu_{d0}}{1 + i\omega/\omega_d} \quad (3)$$

, where μ_{s0} and μ_{d0} are the permeability of spin and domain wall at DC respectively, ω_s and ω_d are the relaxation frequency of the spin and the domain wall. Fig. 3 shows the permeability of CMD10 at room temperature (10°C).It is seen that the permeability has very strong frequency dependence and becomes small at 2~3GHz under considering. The measured number at 2GHz is ε=12.5(±0.7)+i0 and μ=1.3-i7.

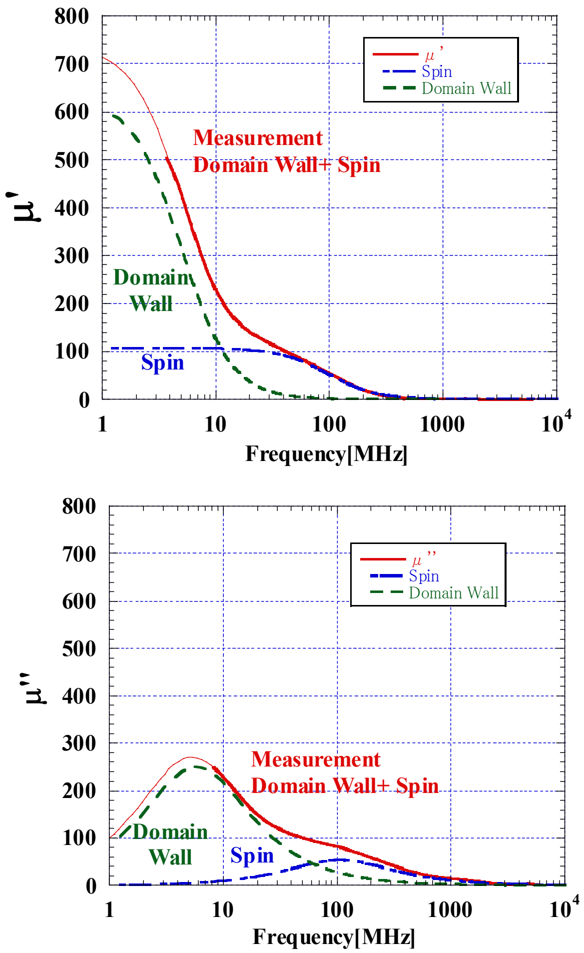

Fig. 3: the permeability of CMD10 at room temperature (10°C)

HOM Q-values measured by single cell DDC agreed with the CST-studio simulation result using these measured parameters at room temperature (Table 1). Thus, we convinced the measurement method. The Q-values are magnitude of 1~2 smaller than that of TESLA type HOM Coupler. Since we put the ferrite at 80K location, the temperature dependence has to be considered.

Table 1: HOM-Q in DDC single cell

Mode	Measurement	Simulation
TE111	199	173
TM110	298	273
TM011	Not detected	Not Detected

We measured RF characteristic parameter of the ferrite at low temperature (300K~77K) by immersing the sample holder in liquid nitrogen. Fig. 4 shows the temperature dependence of μ_{s0}, μ_{d0}, ω_s and ω_d of CMD10. The sample temperatures have an error because we measured at the out wall of the sample holder during cooling down/up. However, the 77K in Fig. 4 is accurate, because the sample was in the thermal equilibrium. The measured number at 2GHz is ε=12.0(±0.4)+i0 and μ=1.4-j4.5. The RF dissipation is calculated by the following equation.

$$W = \omega \oint HdM = \frac{1}{2}\omega H_m \mu'' = \frac{1}{2}\omega H_m \mu' \tan\delta \quad (4)$$

The RF dissipation at 77K is more than half at room temperature, and it can function enough for our purpose.

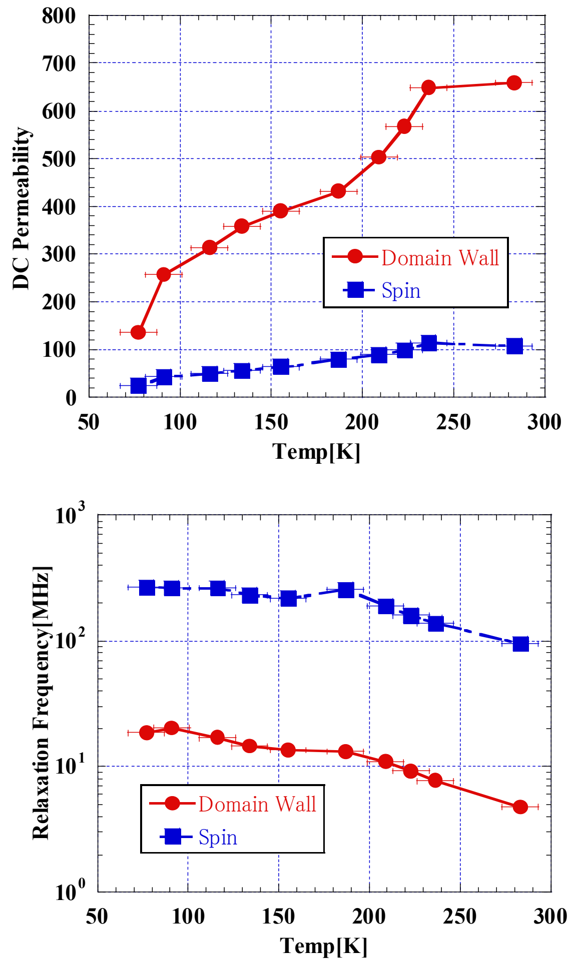

Fig. 4: Temperature dependence of CMD10

RF Design for Absorber of the DDC

We designed the RF absorber geometrical shape by using the ferrite measured RF characteristic at liquid nitrogen temperature. We simulated the reflection power from the coaxial waveguide (outer diameter is Φ80, inner diameter is Φ60) with absorber at the terminal (Fig.5 (a)). Harmful HOMs are distributed at 2~3GHz in ILC 1.3GHz cavities.

We designed for the absorber geometrical shape to have a minimum reflection at these frequencies. Fig. 5 (b) is an example of the simulation, of which condition is outer diameter and length of absorber are fixed and inner diameter is changed. We decided the absorber shape as outer diameter is Φ196mm, inner diameter is Φ170mm and length is 20mm. considering for easy fabrication.

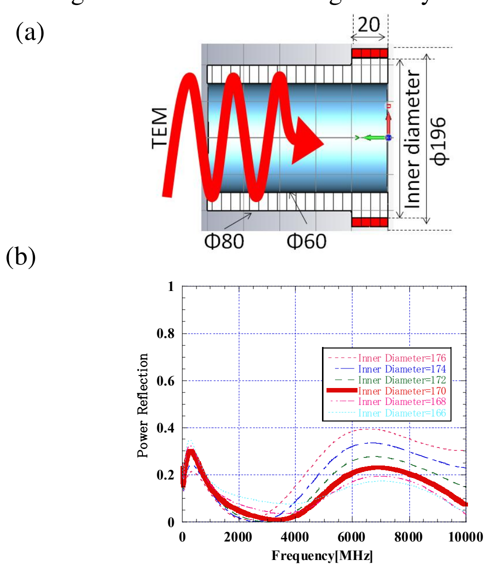

Fig. 5: Frequency dependence of the reflection power and absorber shape a) Coaxial waveguide for the simulation b) Frequency vs. reflection power in the case at outer diameter and length of absorber fixed.

Thermal Structure for the DDC

In ILC cryomodules, only accelerating cavity is cooled, the others are out of the He vessel. To suppress the cryogenic load, we have to reduce heat flux to 2K system. We designed that the HOM dissipation heat flux conducts to 80K thermal shield, and not to conduct to 2K.

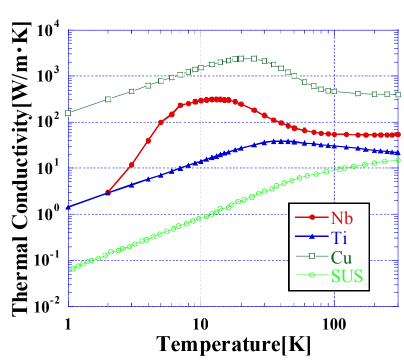

Fig. 6: Thermal conductivity of Nb, Ti, Cu and SUS

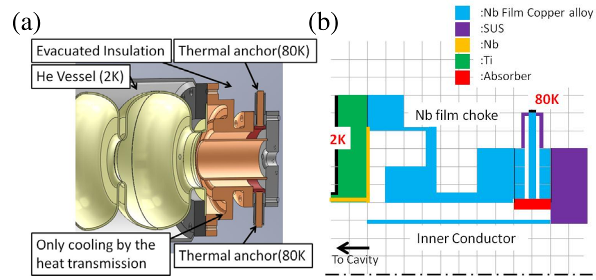

Fig.7: Thermal condition and structure.

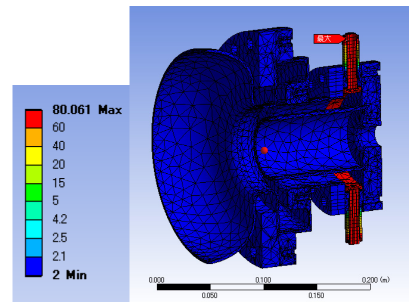

Fig 8: Temperature distribution in DDC.

Fig.6 shows the thermal conductivity of Nb, Ti, Cu and SUS [7, 8] for used material in this design. There are three features in this DDC thermal structure design. One is that inner conductor made of Nb film coated on pure copper [9] and the choke made of Nb film coated on copper alloy (NC50; Yamatogokin Co. Ltd. [10]), because these are kept at 2K. Second feature is that 80K thermal anchors are connected to stainless flange with low thermal conductivity, for the heat flux not to conduct to 2K system. Third feature is absorber flange. It is made of NC50 to make the heat transfer efficient between choke and inner conductor. Fig. 7 shows the DDC thermal structure. Fig. 8 shows the static state simulation result. Inner conductor can be kept at 2.1K and heat flux from 80K to 2K is 20mW. It is the same value of ILC baseline cavity design. We designed the thermal structure consistent with well conducting of HOM dissipated power to 80K and insulating from 2K system.

9 CELL DDC

We could reduce enough Q-values of HOMs on Single Cell DDC as shown in Table 1. In this section, we apply the DDC to 9 cell cavity. In ILC, Q-values of HOMs should be smaller than 10^5 [11].

9 cell DDC type-1

When we apply the DDC to 9 cell cavity, we have to put choke at one side, because the input coupler will be mounted on the other side. Thus, simple DDC loses the mirror symmetry on the beam axis. Fig. 9 shows the simple 9 cell DDC (type-1). Some HOMs (TE111-1/9π mode (Mode Number =28)) weakly couples with DDC as shown in Fig. 10.

These Q-values of HOMs are higher than ILC target. In addition all TM010 pass-band modes look high Q-values compared to ILC cavity. However there R/Q-values are compatible with that of ILC design therefore they are not so problematic. The problem is in the high Q TE111 and others. Fig. 11 shows HOM Q of type-1 compared with TESLA [12] and STF baseline cavities [13].

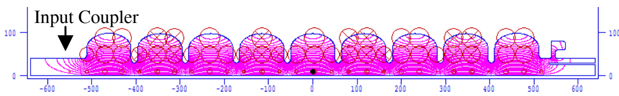

Fig 9: 9 Cell DDC Type-1.

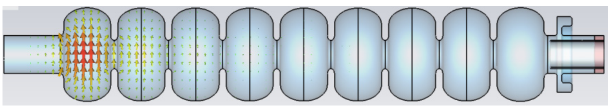

Fig 10: Electric Field distribution TE111-1/9π Mode.

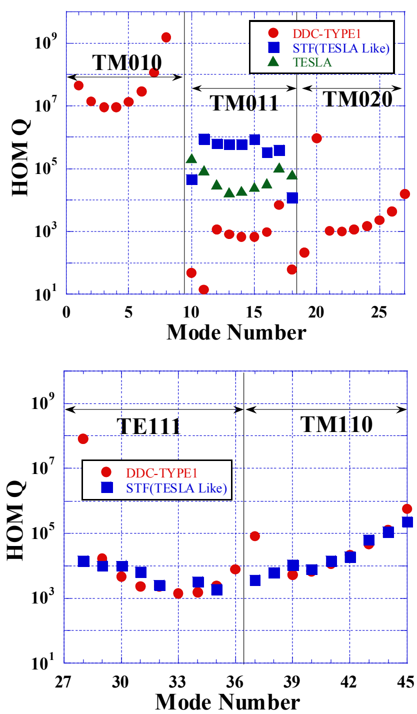

Fig 11: HOMs Q of 9Cell DDC Type-1, TESLA、STF Baseline.

9 Cell DDC Type-2

In 9cell DDC, if the mirror symmetry recovers, the Q-values of HOMs will be low. We simulate type-2 (Fig.12), which input coupler side is coaxial symmetry. Fig13 shows HOMs Q of type-2. Q of TE111-1/9π mode (Mode Number=28) is much smaller than the type-1. However, type-2 is not optimized well, Q of TM020-1/9π mode still high. We hope to achieve lower Q-value of HOMs with 9Cell than that of TESLA type HOM coupler, if it will be optimized well.

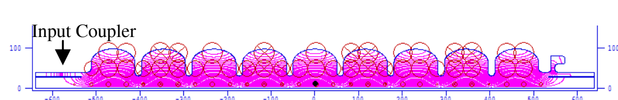

Fig. 12: 9Cell DDC Type-2.

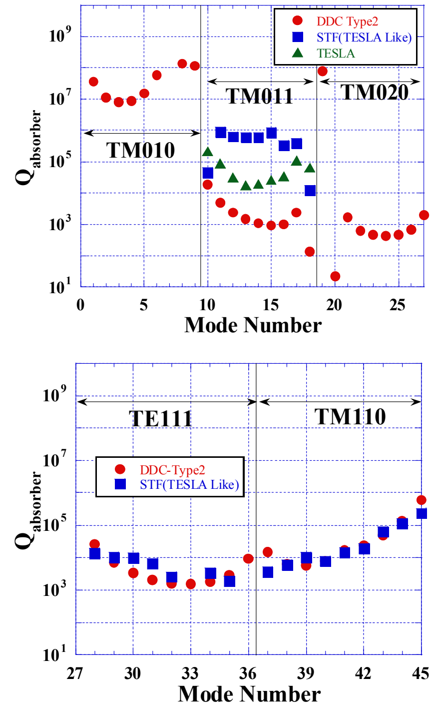

Fig 13: HOM Q of 9Cell DDC Type-2, TESLA and STF Baseline.

SINGLE CELL DDC

The other target of DDC is high field accelerating cavity. We have started the vertical test of the single cell DDC without inner conductor. The accelerating cavity and choke cavity were made of large grain niobium. We assembled the cavity using the indium well established seal first, which is to separate leak problem at seal and DDC cavity characteristics, if you confirmed DDC cavity characteristic we go ahead the MO seal. Fig. 15 is a very preliminary result of the vertical test. The Q-value is very low, which might be related to the beam tube structure or RF contact at seal position. The reason is that the surface magnetic field at the seal is 1/6 of maximum surface magnetic field of the cavity. It is not so low field (Fig. 14). We have to solve this issue soon.

Fig. 14: Single Cell DDC.

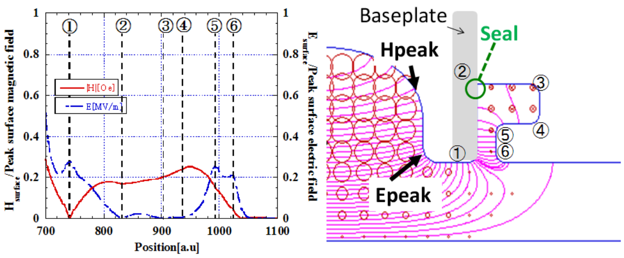

Fig. 15: Surface RF field of DDC without inner conductor.

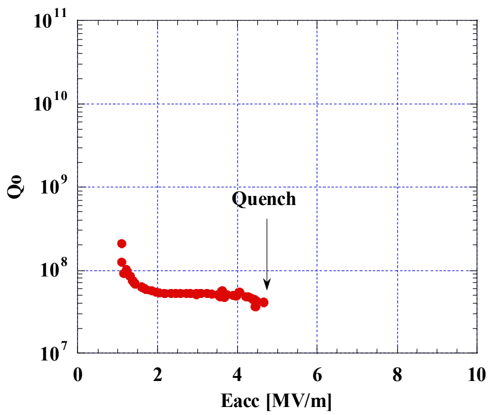

Fig. 16: Vertical test result of Single Cell DDC without inner conductor.

SUMMARY

We measured the parameter of the Ni-Zn ferrite at low temperature. We designed the best absorber shape for the DDC. We simulated the 9Cell DDC shape. It turn out that the large mirror symmetry break is an issue. We have started the vertical test of the single cell DDC.

REFERENCES

[1] M. Dohlus, et al., “Coupler kick for very short bunches and its compensation”, Proceedings of EPAC08, Genoa, Italy, MOPP013, p.580.

[2] F. Furuta, et al., “High Field Q-slope problem in end group cavities”, Proceedings of 10th EPAC2006, Edinburgh, June 2006, p. 750.

[3] http:// www.cmi-ferrite.com

[4] A. M. Nicolson, et al., “Broad-Band Microwave Transmission Characteristics from a Single Measurement of the Transient Response”, IEEE TRANSACTIONS ON INSTRUMENTATION AND MEASUREMENT, VOL. IM-17, NO. 4, DECEMBER 1968.

[5] A. J. Peacock, “Hand Book of polyethylene”, CRC Press, 2000.

[6] T. Tsutaoka, “Frequency dispersion of complex permeability in Mn–Zn and Ni–Zn spinel ferrites and their composite materials”, J. Appl. Phys. 93, 2789 (2003).

[7] http://riodb.ibase.aist.go.jp/TPDB/AJAX/

[8] F. Koechlin, “Parameterization of the niobium thermal conductivity in the superconducting state”, Supercond. Sci. Technol. 9. 453 (1996).

[9] R. Russo, “Quality measurement of niobium thin films for Nb/Cu superconducting RF cavities”, Meas. Sci. Technol. 18, 2299(2007).

[10] http://www.yamatogokin.co.jp/

[11] ILC-RDR, http://lcdev.kek.jp/RDR/.

[12] J. Sekurowicz, “Higer order mode coupler for TESLA”, Proceedings of 6th SRF 1993 p. 426.

[13] K. Watanabe, “New HOM coupler design for ILC superconducting cavity”, Nucl. Instr. and Meth. A 595 (2008) 299.